Properties of intermediate width structure in $^{12}C(^{12}C,^{12}C)^{12}C(0_2^+)$

S. F. Pate, R. W. Zurmühle, P. H. Kutt, and A. H. Wuosmaa
Tandem Accelerator Laboratory, University of Pennsylvania, Philadelphia, Pennsylvania 19104
(Received 7 December 1987)

We have made detailed angular distribution measurements for the inelastic scattering channel $^{12}C(^{12}C,^{12}C)^{12}C(0_2^+)$ in the region of a known prominent structure at $E_{c.m.}=29.0$ MeV. Our analysis shows that the two partial waves $l=16\hbar$ and $18\hbar$ contribute significantly to this structure. The width and centroid of the contribution from the dominant l value, $18\hbar$, are identical to those of a structure seen in the inelastic 2^+ channel.

I. INTRODUCTION

Many heavy-ion systems are now known to exhibit structure in their excitation functions. The most extensively studied of these systems is the one in which these phenomena were first discovered, $^{12}C+^{12}C$. In fact, the experimental techniques, methods of analysis, and vocabulary used to study the resonances of $^{12}C+^{12}C$ scattering form the paradigm for the investigation of all other heavy-ion systems.

In a recent paper, Ordoñez *et al.*[1] have shown that the intermediate structure observed in elastic scattering between $E_{c.m.}=5.5$ and 33 MeV (and from $l=0\hbar$ to $16\hbar$) can be explained by a double minimum optical potential, suggesting a picture of two ^{12}C nuclei rotating about one another in a molecular configuration. Extensive work on structure in inelastic channels, particularly on the single 2^+ and mutual 2^+-2^+ excitations, has also been done. These are seen to be correlated with the resonances in the elastic channel. Groups of resonances with the same sign are clustered about energies which correspond to maxima in the fusion cross section for $^{12}C+^{12}C$.[2] This suggests that the intermediate structure arises from fragmentation of the gross structure seen in the fusion channel. The picture of fragmented gross structure is also seen in the resonances of heavier systems; for example, $^{24}Mg+^{24}Mg$ (Ref. 3) and $^{28}Si+^{28}Si$ (Ref. 4).

Scattering in $^{12}C+^{12}C$ to the single excitation of the 0_2^+ (7.654 MeV) state of ^{12}C also provides an interesting challenge. This channel is strongly momentum mismatched and only rather weakly excited. A structure at $E_{c.m.}=28.5$ MeV reported by Fulton, Cormier, and Herman[5] at Rochester is well correlated in energy with a structure in the 3^- exit channel, but not so well correlated with structures in the 2^+, 2^+-2^+, and 4^+ exit channels centered around $E_{c.m.}=30.0$ MeV. Fulton *et al.*[6] measured angular distributions at five beam energies across this structure. They concluded that the structure is not a resonance but possibly results from barrier matching effects. This is shown in distorted-wave Born-approximation (DWBA) calculations using a folding-model prescription. Unfortunately, although they fit the general features of the excitation function, they do not reproduce the angular distributions well at all; the fit to the distribution at the peak of the structure, for example, is completely out of phase with the data. They suggest that the dominant spin may be $l=16\hbar$, but also warn that this result is sensitive to the choice of DWBA parameters. Their calculation predicts the occurrence of additional structures at energies $E_{c.m.}=24$ and 33 MeV. The absence of these structures in the data is blamed on the small range of angles covered ($\theta_{c.m.}=30°-50°$). Because of these unresolved issues, we decided to perform more detailed angular distribution measurements covering an angular range as large as possible over the energies surrounding the structure in order to obtain information about the angular momenta involved in the scattering.

II. DATA ACQUISITION

Angular distributions for the $^{12}C(^{12}C,^{12}C)^{12}C(0_2^+)$ reaction were measured at energies $E_{c.m.}=26.5-30.5$ MeV in 0.5 MeV steps, using a large solid angle ΔE-E telescope. These energies cover the region of the peak reported by Fulton *et al.*[5] For all energies, measurements were made for $\theta_{c.m.}=30°-100°$. At the three energies $E_{c.m.}=28.0$, 28.5, and 29.0 MeV, the distributions were measured up to $\theta_{c.m.}=20°$. The analysis of the data impressed on us the need for additional forward angle distribution data; we then obtained data up to $\theta_{c.m.}=10°$ at all energies using a magnetic spectrograph.

A. Telescope runs

Our ΔE-E telescope consists of a gas ionization chamber with axial charge collection followed by a position sensitive 50-detector array constructed on a single silicon wafer. A cross section of this device is shown in Fig. 1. A similar device has been described in detail in an earlier publication.[7] One major improvement shown here is the introduction of two rectangular frames serving as field shaping electrodes. The front electrode is electrically connected to the window while the rear electrode is grounded. This configuration generates a more uniform electric field which leads to noticably improved ΔE resolution. The gas used was a mixture of 90% Ar and 10% CH_4, at a pressure of $\frac{1}{4}$ atm. The active length of the gas volume is 15 mm. The entrance window is a 2.5 μm foil of aluminized Mylar. This window, which also serves as the electrode for the ΔE signal, was negatively biased in

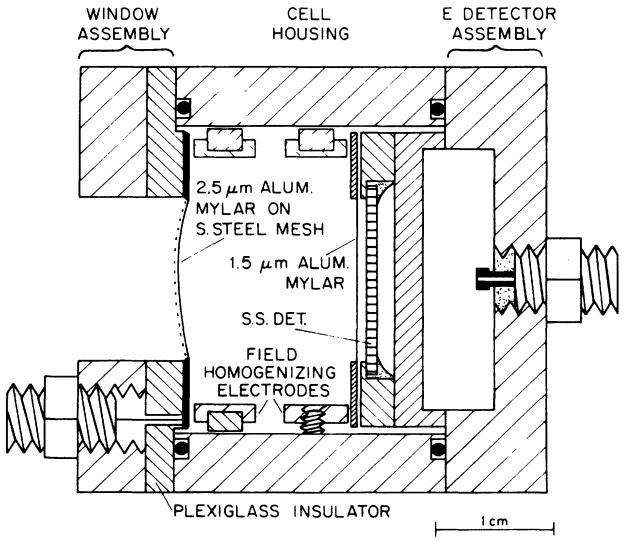

FIG. 1. Cross section of the ΔE-E telescope, showing the field homogenizing electrodes.

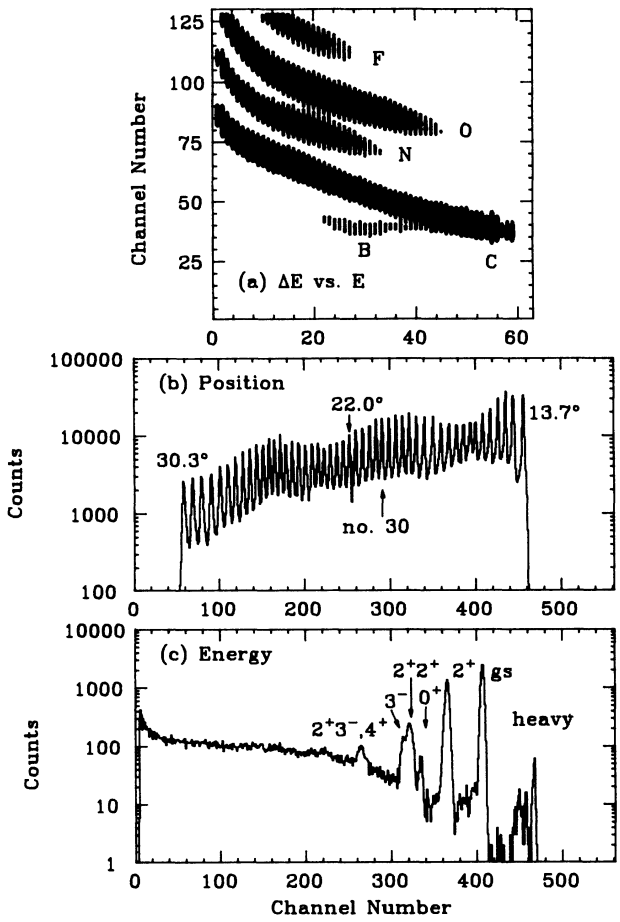

FIG. 2. Spectra from the ΔE-E telescope, taken at $E_{lab}=58$ MeV, and with the telescope centered at $\theta_{lab}=22°$. (a) Particle identification spectrum; groups are labeled by their atomic species. (b) Position spectrum for events from the C group in (a). (c) Energy spectrum for events from the C group in (a) and from the 30th detector element, indicated in (b). Peaks are labeled by their corresponding excited states in ^{12}C. The group labeled "heavy" arises from heavy contaminants in the target.

our experiment to prevent secondary electrons, originating in the target, from reaching the window, where they would have added considerable noise to the ΔE signal. The active area of the silicon wafer is 50×16 mm. At a detector-target distance of 140 mm, the detector has a solid angle of 41 msr, and covers an angular range of 20°. The targets used were self-supporting isotopic ^{12}C foils, 50 $\mu g/cm^2$ thick, corresponding to an energy loss of $\Delta E_{c.m.}\approx 70$ keV. The ^{12}C beam was generated by the University of Pennsylvania Tandem Accelerator. Two monitor counters, at 10° on either side of the beam and of solid angle 0.0081 msr, provided normalization for the experiments via comparison with optical model calculations of the elastic cross section using the Woods-Saxon parameters of Reilly *et al.*[8]

Figure 2 shows typical spectra for the detector taken from a run at $E_{lab}=58$ MeV, with the telescope centered at $\theta_{lab}=22°$. Figure 2(a) is a ΔE-E contour map, showing the variety of ions produced in the experiment. A software gate applied during acquisition eliminated proton and alpha events which would normally appear in the lower end of the ΔE spectrum. Events in the "C" contour were collected into 50 separate energy spectra, one for each detector on the silicon wafer. Figure 2(b) is a position spectrum for C events, and Fig. 2(c) is an energy spectrum for detector no. 30 ($\theta_{lab}=20°$) for these same events. The small cross section for the 0_2^+ state is evident. The energy resolution of the detector was 350 keV full width at half maximum.

The background visible underneath the 0_2^+ peaks arises from low energy tails from the ground state and 2^+ peaks. The tails account for less than 0.1% of the total number of counts in these peaks, but the 0_2^+ cross section is so small that the number of counts in the 0_2^+ peak is usually of similar magnitude as the number in the background beneath it. This background was subtracted by simply drawing a linear background, guided by the level of the background on either side of the peak. In the final angular distributions, counts from adjacent detectors were combined in order to improve statistics. Thus each of the two angle settings of the telescope produced 25 data points, about one per degree (laboratory).

B. Spectrograph runs

A Browne-Buechner single focusing broad-range spectrograph[9] was used for the forward angle measurements. It has a radius of 65 cm and is oriented so as to deflect incoming particles vertically. In the focal plane, centered at a bending angle of 90° and at a trajectory distance of 2.32 m from the target, is a silicon surface barrier detector with continuous position sensitivity and an active area of 100×12 mm. An aperture at a distance of 82.5 mm from the target and of dimensions 12.5 mm (vertical) and 3.2 mm (horizontal) restricted the number of particles entering the magnet, and helped reduce the back-

ground in the spectrograph. A beam collimator was also employed for this purpose. With these improvements we were able to obtain useful data for the 0_2^+ peak for laboratory angles of 5° and larger. Measurements were made for $\theta_{lab}=5°-15°$ in 1° steps, at all energies covered by the telescope runs. A monitor at $\theta_{lab}=20°$ was used to normalize these runs. The targets for these runs were 100 $\mu g/cm^2$ thick ($\Delta E_{c.m.} \approx 140$ keV).

Events were collected into a single 512×512 channel histogram of energy versus position. Figure 3(a) shows an energy spectrum from the run at $E_{lab}=58$ MeV and $\theta_{lab}=9°$. Figure 3(b) is a position spectrum for events in the region around the ^{12}C peak in the spectrum of Fig. 3(a). The 2^+-2^+ and 3^- peaks are visible on the left of the spectrum, with the 0_2^+ near the middle. The background is from the degraded beam particles, and was subtracted. For angles smaller than 5° this background becomes so large as to prevent observation of the small 0_2^+ peak.

III. DATA ANALYSIS

The angular distributions are displayed in Fig. 4. Figure 5(a) shows our angle integrated cross section as a function of energy, for our full angle range ($\theta_{c.m.}=10°-90°$), as well as the same angle range as Ref. (5) ($\theta_{c.m.}=30°-50°$), along with the data of Ref. (5). The latter two sets of points agree in their shapes, but there is a normalization difference of a factor of about 1.5. The centroid of the structure in the full angle range data is placed at a slightly higher energy than in the limited angle range data. In our data a discontinuity in the cross section is present at $E_{c.m.}=29.0$ MeV for the full angle range, and is suggested as well in the narrow angle range data. This may suggest the existence of structure that is narrower than our step size of $\Delta E_{c.m.}=0.5$ MeV, a point to which we shall return.

Because in the $^{12}C(^{12}C,^{12}C)^{12}C(0_2^+)$ reaction the entrance and exit channels have zero spin, the angular dependence of the cross section will have the form

$$\sigma(\theta)=\left|\sum_l a_l P_l(\cos\theta)\right|^2 , \quad (1)$$

where the P_l are Legendre polynomials of order l and the a_l are complex numbers. To obtain some guidance about the range of angular momenta that strongly contribute to the cross section, we can compare the experimental angular distributions with single squared Legendre polynomials. To this purpose Fig. 6 shows the angular distribution for $E_{c.m.}=29$ MeV, with P_{16}^2 and P_{18}^2 superposed. This

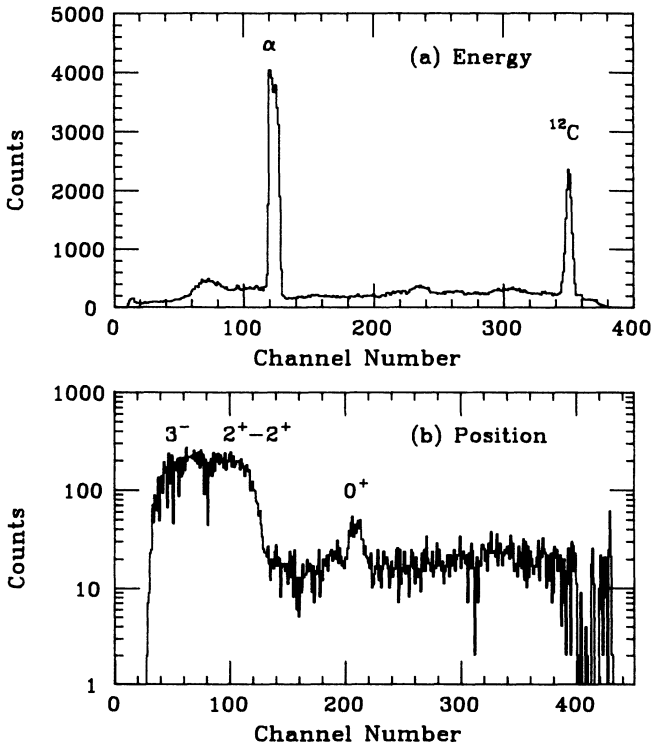

FIG. 3. Spectra from the magnetic spectrograph, taken at $E_{lab}=58$ MeV and $\theta_{lab}=9°$. (a) Energy spectrum, showing α and ^{12}C peaks. (b) Position spectrum for ^{12}C events.

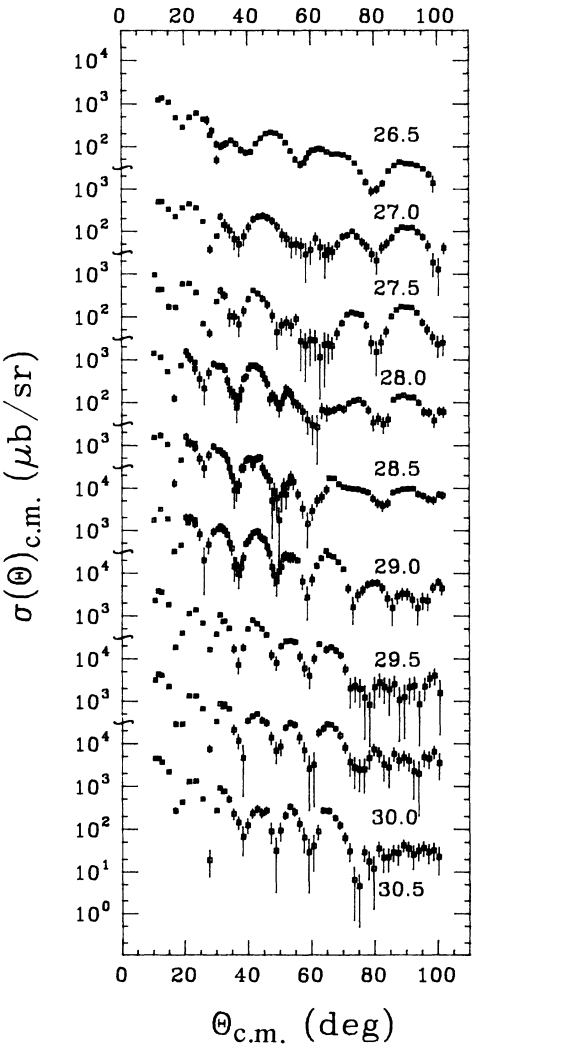

FIG. 4. Angular distributions for the $^{12}C(^{12}C,^{12}C)^{12}C(0_2^+)$ reaction; each distribution is labeled by the center of mass energy, in MeV.

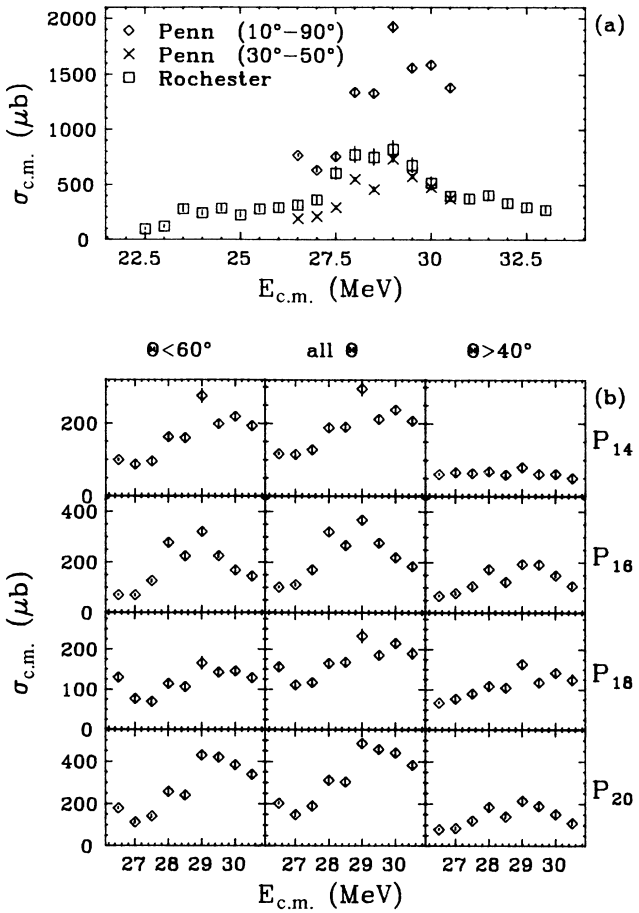

FIG. 5. Angle integrated cross sections. (a) Integrated cross sections for our data are shown for our full angular range, as well as an angle range equal to that of Ref. 1. The data of Ref. 1 are also shown. (b) Integrations at the zeros of Legendre polynomials, as explained in the text.

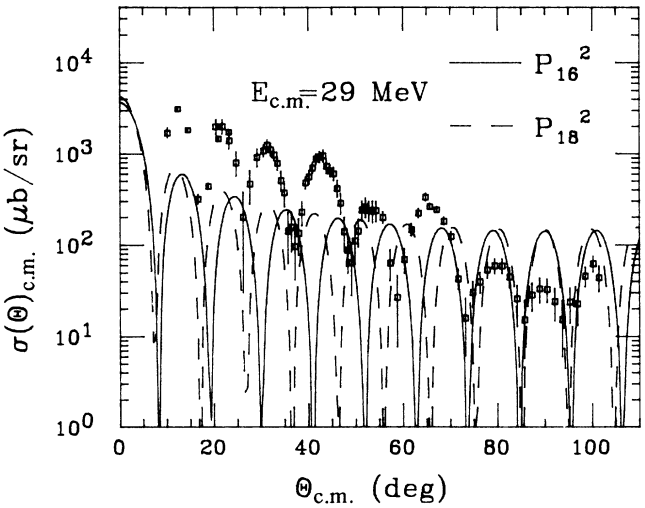

FIG. 6. Angular distribution for $E_{c.m.}=29.0$ MeV, with curves corresponding to P_{16}^2 (solid line) and P_{18}^2 (dashed line) superposed. The normalization of each curve was chosen to best fit the data.

energy has the highest integrated cross section and an angular distribution with clearly pronounced oscillations. There are eight minima between 0° and 90° (we did not actually reach the most forward of these in our spectrograph runs, but its existence is clearly indicated by the data). This would normally imply the dominance of $l=16\hbar$, but the forward angle minima are out of phase with those of this angular momentum. In fact, the forward angle minima are perfectly in phase with $l=18\hbar$. Interference with direct, nonresonant processes clearly plays an important role. According to Ordoñez *et al.*,[1] the dominant spin in the elastic channel at this energy is probably $l=16\hbar$. Optical model calculations, using the same potential as for our normalizations, indicate that the entrance channel grazing angular momentum is about $16\hbar-18\hbar$. The same potential predicts $l=14\hbar$ for the grazing angular momentum in the 0_2^+ exit channel.

A different method that uses the minima of a measured distribution to study the spin of resonances has been employed by Parker *et al.*[10] to study elastic scattering in $^{12}C+{}^{12}C$ between 17.5 and 21.5 MeV and by Balamuth *et al.*[11] to study the inelastic scattering of $^{16}O+{}^{16}O$ between 17 and 41 MeV. The method involves integrating the cross section only over angles in the vicinity of the zeroes of a particular Legendre polynomial. If a resonance or structure is dominated by the chosen polynomial, then the energy dependence of such an integral will *not* have peaks at the energies which correspond to resonances of the given angular momentum; the trend should be flat. This provides a model independent method of determining the dominant angular momenta, since no assumptions are made concerning which values of l to include in the analysis. The only adjustable parameters involved are the width of the region of integration around each zero and the choice of which region of the distribution to use (forward angles, back angles, all angles). The latter can affect the the sensitivity of this method; for example, if the forward angle region is dominated by a scattering process not related to the resonance scattering, the sensitivity might be increased through omission of the forward angle minima.

In our analysis we tried three different angle ranges. One set of integrations was performed using the full angular range (10°–90°), another using only the data forward of 60°, and another using data backward of 40°. The width of the region around each zero was chosen to be 2°. Figure 5(b) displays the results of these integrations for $l=14\hbar$, $16\hbar$, $18\hbar$, and $20\hbar$. The $l=14\hbar$ integration for back angles is very flat, but it shows marked structure when the full angular range is considered. This agrees with our simple observation that the spacing of the minima of the 29.0 MeV distribution increases at back angles. All of the $l=18\hbar$ integrations are suppressed in the region of the peak (29.0 MeV), relative the other l's. This indicates that $l=18\hbar$ makes the largest contribution to the structure in this energy region.

To get more detailed information concerning the energy-dependent behavior of the dominant momenta, it is necessary to perform a coherent partial wave decompo-

sition of the data. This involves fitting the data to a function of the form of Eq. (1). In performing our fits, we only considered contributions from $l=12\hbar$, $14\hbar$, $16\hbar$, and $18\hbar$. A minimization program MINUIT from CERN (Ref. 12) was used to find the values of the a_l's that best fit (least-squares) the data. Because the results of such a fitting procedure are not unique (the a_l's enter the fitting function nonlinearly), we tried a variety of initial conditions in order to find those conclusions about the data which are independent of the fitting procedure. One method was to fit one energy starting from initial conditions which were "far" from the actual shape of the data, and to use the results of this fit as the initial conditions for the fits to the adjacent energies, and so on. Chains of fits of this sort were performed starting at 21.5 MeV and going up, starting at 30.5 MeV and going down, and also starting at 29.0 MeV and going out. Fits were also performed using "far" initial conditions for every energy. The results for the amplitudes for each angular momentum were very similar (sometimes the same) for each initial condition arrangement. Figure 7 shows the partial cross sections for each angular momentum as given by one of these sets of fits; Fig. 8 shows the fit to the data for each energy. The partial cross sections reveal what we expected after looking at Fig. 6; the largest contributions in the area of the enhancement come from $l=16\hbar$ and $18\hbar$. The contribution from $l=18\hbar$ is the larger of the two, in agreement with the zeros integration analysis carried out above. It is interesting to note that the $l=16\hbar$ cross section experiences a sharp maximum at 29.0 MeV, while the behavior of $l=18\hbar$ is smoother in this region. This occurred in all of the fits. This suggests that if the sharp peak at 29.0 MeV is the result of narrow structure, then the spin of this structure is $16\hbar$, while the spin of the underlying broader structure would be dominated by $18\hbar$. However, with the present energy resolution of these data, such an argument cannot be made very forcefully.

Another measure undertaken to study effects arising from the nonuniqueness of the fits was to generate additional sets of fits using lower l values, in addition to the partial waves discussed above. In one set $l=10\hbar$ was included, and in another set $l=8\hbar$ and $10\hbar$ were included. The inclusion of these lower partial waves did not significantly change the results at the higher energies; $l=16\hbar$ and $18\hbar$ remain the dominant partial waves. However at the three lowest energies, where our fits with only $l=12\hbar$–$18\hbar$ are somewhat inferior to those at the higher energies, some improvement was obtained. In these fits the lowest partial wave always became dominant at the expense of $l=12\hbar$ or $10\hbar$, but the higher partial waves $l=14\hbar$, $16\hbar$, and $18\hbar$, which did not contribute

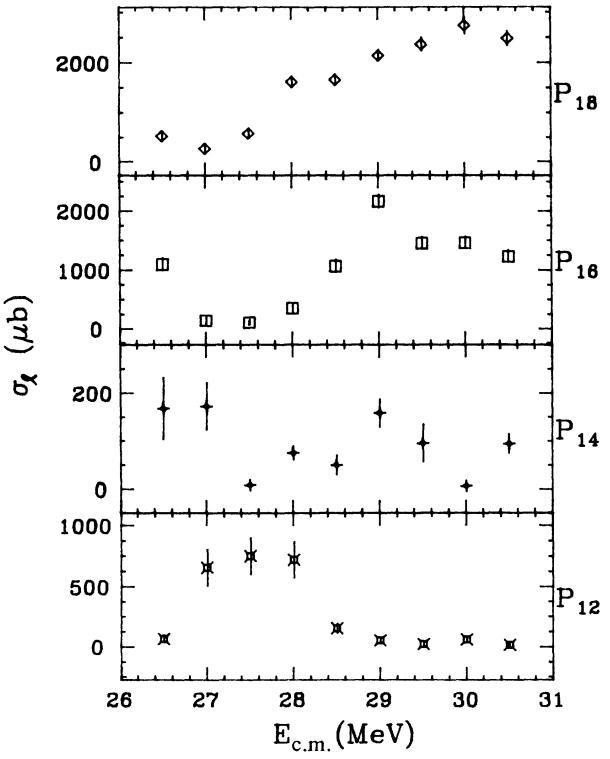

FIG. 7. Partial cross sections $[\sigma_l=4\pi|a_l|^2/(2l+1)]$ for $l=12\hbar$, $14\hbar$, $16\hbar$, and $18\hbar$ from the coherent Legendre polynomial fits.

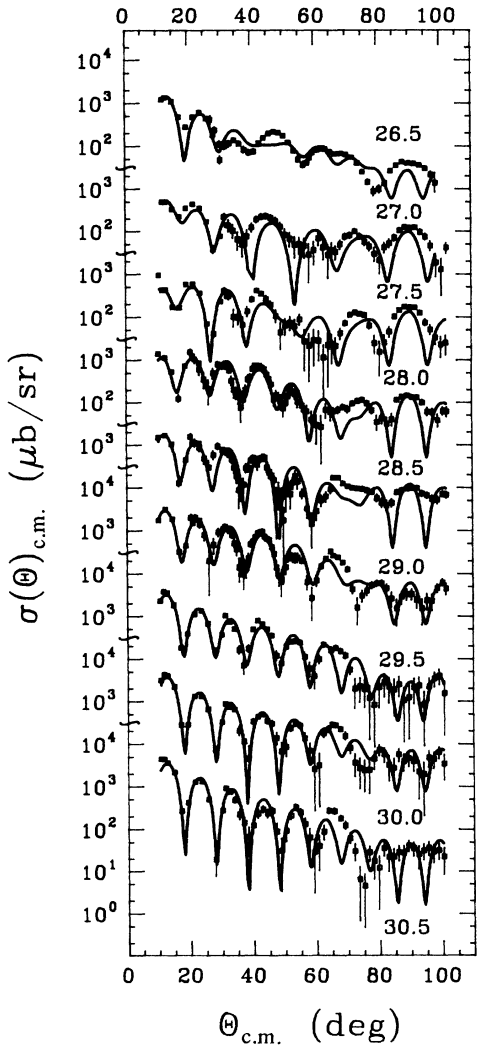

FIG. 8. Angular distributions as in Fig. 4, with fits superposed.

significantly at these lower energies, remained relatively unaffected.

IV. SUMMARY AND CONCLUSIONS

Our measurements seem to point to a picture somewhat different from that of Fulton *et al.*[6] concerning the origin of structure in the $^{12}C(^{12}C,^{12}C)^{12}C(0_2^+)$ reaction around $E_{c.m.}=29.0$ MeV. Whereas Fulton *et al.* indicate that the structure is caused by barrier matching effects, their calculations do not reproduce their angular distributions. Our detailed angular distribution studies show that satisfactory fits can only be obtained for the data in this region with an enhancement of both the $l=16\hbar$ and $18\hbar$ partial waves. They also reveal the possible presence of a narrower structure which is dominated by $l=16\hbar$. It is very surprising that a partial wave as high as $l=18\hbar$ should contribute to this structure because this l value is strongly mismatched in the exit channel. One fascinating aspect of our analysis is the fact that the $l=18\hbar$ partial cross section seems to peak at 30.0 MeV and that it resembles in position and width very closely the structure seen in the inelastic channel to the 2^+ (4.44 MeV) state. This structure was initially thought to have spin $16\hbar$.[2] But this result was deduced mostly from the general systematics of structures in the 2^+ inelastic channel. More recent theoretical[13] and experimental[14] studies indicate that $l=18\hbar$ is a more likely choice. Therefore it is quite possible that the structures seen in these two channels at this energy have the same origin. Of course, the absolute cross sections in the two channels are very different, with the 0_2^+ channel being suppressed by more than one order of magnitude.

There are theoretical grounds for pursuing studies of this structure in terms of resonance behavior, as indicated by the calculations of Marsh and Rae.[15] Using a cranked alpha-cluster model for ^{24}Mg, they have found that two bands, one based on a chain of six alphas, the other on a planar configuration of two rows of three alphas saddled next to each other, overlap at $l=16\hbar-18\hbar$ and $E_{c.m.}=29.0$ MeV. This corresponds to the centroid of the structure when looked at in the large angle range. Mixing of these two configurations could presumably generate a configuration that decays both into the 2^+ (4.44 MeV) and 0_2^+ (7.65 MeV) inelastic channels. However, several questions remain unanswered. It is still not clear why no additional structures are formed at lower energies in the 0_2^+ excitation function. The nature of the $l=16\hbar$ contribution to the present structure is also not fully understood. More experimental measurements to determine the width of any possible fine structure at 29.0 MeV, and dynamical calculations to help explain the nature of any found, are clearly in order.

ACKNOWLEDGMENTS

We would like to acknowledge the assistance of R. Yu, J. Richardson, J. Ma, and S. Saini in the acquisition and analysis of these data. We would like to thank D. P. Balamuth and C. M. Laymon for many helpful discussions, and R. Gilman for providing the MINUIT program. We gratefully acknowledge the financial support of the National Science Foundation.

[1] C. E. Ordoñez, R. J. Ledoux, and E. R. Cosman, Phys. Lett. B **173**, 39 (1986).

[2] T. M. Cormier, C. M. Jachcinski, G. M. Berkowitz, P. Braun-Munzinger, P. M. Cormier, M. Gai, J. W. Harris, J. Barrette, and H. E. Wegner, Phys. Rev. Lett. **40**, 924 (1978).

[3] R. W. Zurmühle, P. Kutt, R. R. Betts, S. Saini, F. Haas, and Ole Hansen, Phys. Lett. **129B**, 384 (1983).

[4] R. R. Betts, B. B. Back, and B. G. Glagola, Phys. Rev. Lett. **47**, 23 (1981).

[5] B. R. Fulton, T. M. Cormier, and B. J. Herman, Phys. Rev. C **21**, 198 (1980).

[6] B. R. Fulton, J. S. Lilley, R. Lindsay, M. A. Nagarajan, N. Rowley, R. Shyam, T. M. Cormier, and P. M. Stwertka, Phys. Lett. **136B**, 322 (1984).

[7] R. W. Zurmühle and L. Csihas, Nucl. Inst. Meth. **203**, 261 (1982).

[8] W. Reilly, R. Wieland, A. Gobbi, M. W. Sachs, and D. A. Bromley, Nuovo Cimento A **13**, 897 (1973).

[9] C. P. Browne and W. W. Buechner, Rev. Sci. Instrum. **27**, 899 (1956).

[10] R. A. Parker, A. D. Frawley, and L. C Dennis, Phys. Rev. C **32**, 1563 (1985).

[11] D. P. Balamuth, T. Chapuran, C. M. Laymon, W. K. Wells, and D. P. Bybell, Phys. Rev. Lett. **55**, 2842 (1985); T. Chapuran *et al.*, Phys. Rev. C **34**, 2358 (1986).

[12] F. James and M. Roos, Comp. Phys. Commun. **10**, 343 (1975).

[13] O. Tanimura, R. Wolf, and U. Mosel, Phys. Lett. **120B**, 275 (1983).

[14] Y. Sugiyama, N. Shikazono, Y. Tomita, H. Ikezoe, T. Tachikawa, E. Takekoshi, S. Kubono, and M. Tanaka, Phys. Lett. **159B**, 90 (1985).

[15] S. Marsh and W. D. M. Rae, Phys. Lett. B **180**, 185 (1986).